
Modified Virtual Impedance Control to Improve Real and Reactive Power Output in Islanded Microgrid

Pradeep Kumar Singh and Dharmendra Kumar Dheer*

*Electrical Engineering Department, National Institute of Technology,
Patna, India*

E-mail: dkdheer@nitp.ac.in

**Corresponding Author*

Received 11 January 2022; Accepted 11 March 2022;
Publication 09 December 2022

Abstract

In this paper, modified virtual impedance control technique is proposed to bring back the sum of real power and reactive power output of all the distributed generators (DGs) to the nominal value. The value of real and reactive power output falls down in the conventional virtual impedance control technique for reactive power sharing improvement in islanded microgrid. The proposed technique modifies the d-axis component of virtual impedance voltage which in turns brings back the sum of real and reactive power output of distributed generators to nominal value keeping achieved reactive power sharing and output voltage intact. The impact of modified virtual impedance technique on the stability of the system is also investigated using eigenvalue analysis. No communication link or optimization technique is required in this work which reduces the complexity of the system making it more reliable and easier to design. The proposed technique works satisfactory for local load as well as the loads which are connected distantly from the distributed generators. The feasibility of the proposed technique is validated in time

Distributed Generation & Alternative Energy Journal, Vol. 38_1, 169–188.

doi: 10.13052/dgaej2156-3306.3818

© 2022 River Publishers

domain simulation in MATLAB/Simulink. The MATLAB R2020b version 9.9 is used in this research work.

Keywords: Islanded microgrid control, reactive power sharing, modified virtual impedance technique, reactive power sharing improvement..

1 Introduction

Distributed energy resources (DERs) are used to provide clean energy which not only helps in meeting the energy demand but also saves the environment. DERs are integrated into the system (either grid connected or islanded microgrid) which are mostly interfaced with the inverters at the front end [1]. Proportional power sharing between the DGs is one of the basic and important criteria for desired operation of DGs in standalone operation. $P - \omega$ and $Q - V$ droop control technique is used to achieve the desired power sharing amongst the DGs [2]. The active power sharing in DGs operating in droop control technique is proportional to rating of DGs but it fails to share reactive power in proportion to the size of DGs. Imprecise reactive power sharing is primarily due to the unequal feeder impedance which needs improvement to avoid circulating current and overloading of smaller DGs.

Various control methods have been proposed in literature for the improvement of reactive power sharing which is reviewed in [3] and can be categorized into: droop-based control technique [4–9] and virtual impedance control technique [10–20]. A self-adjusting nominal voltage-based control method to improve the reactive power (Q) sharing among sources in an islanded microgrid has been proposed in [6] and appreciable improvement in Q sharing has been achieved by adaptive nominal voltage as compared to fixed nominal voltage. An adaptive n_q based method is used in [7] to improve reactive power sharing which uses different value of n_q in different load conditions causing requirement of excessive computation for every change in load. Author in [9] applied communication link for the improvement in power sharing between the DG's. The problem associated with the communication link is that DGs may operate unsatisfactory in case of communication failure or delay in communication.

The basic idea of virtual impedance (Z_v) is to place high value impedance between interfacing converter outputs and the point of common coupling (PCC). This will minimize the impedance mismatch between the DGs and proportional reactive power sharing can be achieved. The value of virtual impedance should be chosen carefully and it should be accurate otherwise it

may affect the stability of the system. To get the accurate value of Z_v [10,11] proposes a strategy to design and implement the virtual impedance. It also suggests a range of virtual impedance with which reactive power sharing can be improved without affecting the system stability. Authors in [14, 15] uses Genetic Algorithm (GA) based optimization and particle Swarm Optimization (PSO) respectively to design virtual impedance controller for reactive power sharing improvement among the DGs. The optimization used increases the computation burden and slows down response of the system. Authors in [16–20] used adaptive virtual impedance method for the improvement of reactive power sharing amongst DGs in islanded microgrid.

Comparative study for the improvement in reactive power sharing among robust droop control strategy (RDCS) and virtual impedance technique is presented in [1]. It is observed that for the higher values of X_v , error in reactive power sharing (Q_{err}) decreases. However, the total sum of active power output (P_{total}) and reactive power output (Q_{total}) of all the sources decreases from the nominal value of the sum of total load connected to the system which is not desirable. In this paper, the conventional virtual impedance technique is modified to reduce the decrement in P_{total} and Q_{total} from its nominal value keeping the achieved reduction in Q_{err} intact.

The organisation of the paper is as follows: Modified virtual impedance control technique and system under study is presented in section-II. Section-III talk over the results obtained in time domain simulation studies. Stability analysis is performed in section-IV. Finally conclusion and scope of future work has been presented in section-V.

2 Modified Virtual Impedance Control and System Under Study

The microgrid is operating in convention droop control scheme for proportional active and reactive power sharing among the sources which is given in (1a) and (1b) respectively.

$$\omega = \omega_n - m_p P \quad (1a)$$

$$V_{od}^* = V_n - n_q Q \quad (1b)$$

where, ω_n and V_n is nominal frequency and voltage respectively. m_p and n_q is active and reactive power droop coefficient respectively. V_{od}^* is d-axis reference output voltage and ω is operating frequency. P is active power output and Q is reactive power output of the source.

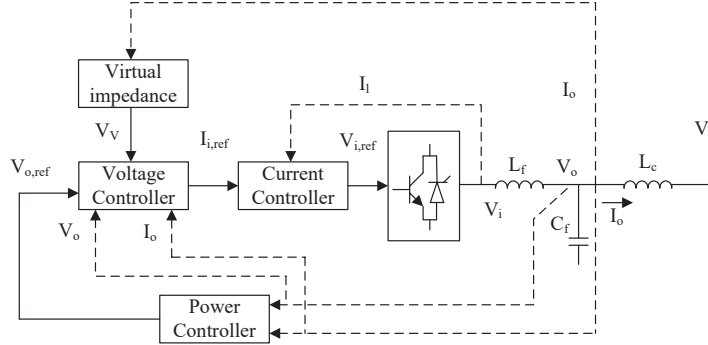


Figure 1 Block diagram of voltage source inverter based DG operating with virtual/modified-virtual impedance control.

The modified virtual impedance control scheme and the system under study are presented in this section.

2.1 Modified Virtual Impedance Control

In this section modified virtual impedance control scheme is introduced which reduces the decrements in P_{total} and Q_{total} as in [1] keeping the achieved reduction in Q_{err} intact.

The conventional virtual impedance control is modified by adding a term $(-X_{v_{add}}I_{od})$ in the d-axis component of virtual impedance voltage (2) to mitigate the effect of decrement in P_{total} and Q_{total} from its nominal value. Algebraic equations corresponding to modified virtual impedance control for V_{vq} and V_{vd} (Figure 2) is proposed as:

$$V_{vd} = R_v I_{od} - X_v I_{oq} - X_{v_{add}} I_{od} \quad (2a)$$

$$V_{vq} = R_v I_{oq} + X_v I_{od} \quad (2b)$$

Where V_{vd} and V_{vq} is d-axis and q-axis component of virtual impedance voltage. R_v and X_v are virtual resistance and virtual reactance respectively. I_{od} and I_{oq} are d-axis and q-axis components of current.

2.2 System Under Study

Line and load data of the microgrid under study (Figure 3) containing three DGs of rating 10kVA each is shown in Table 1 which is adapted from [1].

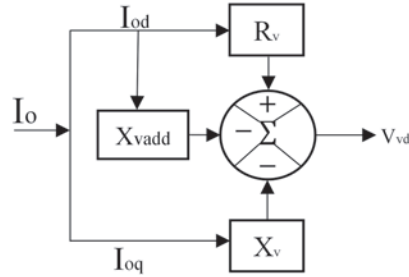


Figure 2 Block diagram of V_{vd} for modified Virtual impedance technique.

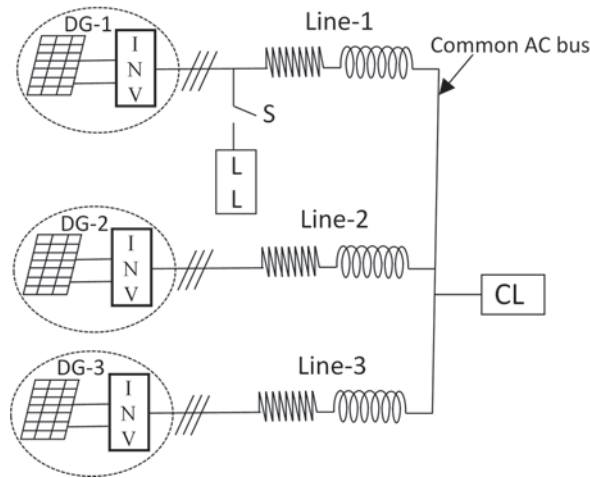


Figure 3 Test system MG1.

Table 1 MG network data

Line no.	Impedance (Ω)	R/X	Load (kVA)
L1	$0.20 + j 0.06$	3.33	CL = $9 + j 4.5$
L2	$0.30 + j 0.09$	3.33	LL = $1.5 + j 0.75$
L3	$0.40 + j 0.12$	3.33	

3 Simulation Results

A comparative study between modified virtual impedance control technique and virtual impedance technique for common load as well as common plus local load (Figure 3) was carried out while the local load is connected at DG_1 .

The values of P , Q , Q_{err} and d-axis output voltage (V_{odr}) is obtained for the different cases which are given as follows:

- Case-1: Varying the X_v from 0.1 to 1.0 Ω in steps of 0.1 Ω while keeping the R_v constant at ($R_v = 0.0 \Omega$) for common load as shown in Table 2.
- Case-2: Keeping R_v and X_v constant at 0.0 Ω and 1.0 Ω respectively while varying the X_{vadd} in terms of X_v for common load as shown in Table 3.
- Case-3: Varying the X_v from 0.1 to 1.0 Ω in steps of 0.1 Ω while keeping the R_v constant at ($R_v = 0.0 \Omega$) for common plus local load as shown in Table 4.
- Case-4: Keeping R_v and X_v constant at 0.0 Ω and 1.0 Ω respectively while varying the X_{vadd} in terms of X_v for common plus local load as shown in Table 5.

3.1 Common Load Case

Based on Table 2 it is found that keeping R_v at $R_v = 0.0 \Omega$ and increasing X_v from 0.1 Ω to 1.5 Ω , causes decrement in reactive power sharing error and improvement in output voltage from $V_{odr} = 0.992$ pu to $V_{odr} = 0.995$ pu. But with increased value of X_v , active power output and average reactive power output also decreases from $P = 2.88$ kW ($R_v = 0.0$, $X_v = 0.1$) to $P = 2.555$ kW ($R_v = 0.0$, $X_v = 1.5$) and $Q_{exp} = 1.42$ kVAr ($R_v = 0.0$, $X_v = 0.1$) to $Q_{exp} = 1.2953$ kVAr ($R_v = 0.0$, $X_v = 1.5$) respectively. Figure 4 also shows that active output power P and average reactive output power Q_{exp} decreases with increased values of X_v which is not desired and needs improvement.

When system is modified by adding an addition term X_{vadd} and increasing its value in terms of X_v there is increment in the output power P as well as average reactive output power Q_{exp} . The output power P improves to $P = 2.92$ kW ($X_{vadd} = X_v/2$) and the average reactive power Q_{exp} improves to $Q_{exp} = 1.4167$ kVAr ($X_{vadd} = X_v/2$) (Table 3). The R_v and X_v is kept constant at 0.0 Ω and 1.0 Ω respectively. Figure 5 also validate the the improvement in active output power P and average output reactive power Q_{exp} after adding the X_{vadd} . It is also observed that reactive power sharing error is almost unchanged and output voltage is maintained at $V_{odr} = 0.995$ pu in this case.

3.2 Common Plus Local Load Case

When the local load is also connected along with common load and varying X_v from 0.1 Ω to 1.5 Ω keeping R_v constant at ($R_v = 0.0 \Omega$), the error

Table 2 Virtual impedance implementation for common load case: $R_v = \text{constant}$, $X_v = \text{variable}$

Virtual impedance (Ω)	$P_{(1-3)}$ (kW)	$Q_{(1-3)}$ (kVAr)	Q_{exp} (kVAr)	$Q_{err(1-3)}$ (%)	$v_{odr(1-3)}$ (pu)
$R_v = 0, X_v = 0.1$	2.88	2.51, 1.35, 0.40	1.42	76.76, -4.93, -71.83	0.992, 0.996, 0.999
$R_v = 0, X_v = 0.2$	2.85	2.21, 1.36, 0.64	1.4033	57.48, -3.08, -54.4	0.993, 0.995, 0.998
$R_v = 0, X_v = 0.3$	2.83	2.03, 1.37, 0.79	1.3967	45.34, -1.90, -43.43	0.993, 0.995, 0.997
$R_v = 0, X_v = 0.4$	2.80	1.91, 1.37, 0.88	1.3867	37.74, -1.20, -36.54	0.994, 0.995, 0.997
$R_v = 0, X_v = 0.5$	2.78	1.81, 1.36, 0.945	1.3717	31.95, -0.85, -31.10	0.994, 0.995, 0.997
$R_v = 0, X_v = 0.6$	2.76	1.74, 1.35, 0.99	1.36	27.94, -0.74, -27.20	0.994, 0.995, 0.997
$R_v = 0, X_v = 0.7$	2.73	1.685, 1.345, 1.025	1.3517	24.66, -0.50, -24.16	0.994, 0.995, 0.996
$R_v = 0, X_v = 0.8$	2.71	1.635, 1.335, 1.05	1.34	22.01, -0.37, -21.64	0.994, 0.995, 0.996
$R_v = 0, X_v = 0.9$	2.69	1.595, 1.325, 1.068	1.3293	19.99, -0.32, -19.67	0.995, 0.996, 0.996
$R_v = 0, X_v = 1.0$	2.665	1.555, 1.31, 1.08	1.315	18.25, -0.38, -17.87	0.995, 0.996, 0.996
$R_v = 0, X_v = 1.1$	2.64	1.525, 1.303, 1.09	1.306	16.77, -0.23, -16.54	0.995, 0.996, 0.996
$R_v = 0, X_v = 1.2$	2.618	1.492, 1.290, 1.095	1.2923	15.45, -0.18, -15.27	0.995, 0.996, 0.996
$R_v = 0, X_v = 1.3$	2.595	1.468, 1.28, 1.1	1.2827	14.44, -0.21, -14.23	0.995, 0.996, 0.996
$R_v = 0, X_v = 1.4$	2.575	1.442, 1.268, 1.102	1.271	16.45, -0.27, -13.18	0.995, 0.996, 0.996
$R_v = 0, X_v = 1.5$	2.555	1.418, 1.257, 1.103	1.2953	12.60, -0.18, -12.42	0.995, 0.996, 0.996

Table 3 Variation in $X_{V_{add}}$ keeping $R_V = 0.0$ and $X_V = 1.0$ for common load case

$X_{V_{add}}$ (Ω)	$P_{(1-3)}$ (kW)	$Q_{(1-3)}$ (kVAr)	Q_{exp} (kVAr)	$Q_{err(1-3)}$ (%)	$v_{odr(1-3)}$ (pu)
$\frac{X_V}{10}$	2.70	1.58, 1.33, 1.095	1.335	18.35, -0.375, -17.975	0.995, 0.996, 0.996
$\frac{X_V}{9}$	2.71	1.58, 1.33, 1.097	1.336	18.26, -0.449, -17.889	0.995, 0.996, 0.996
$\frac{X_V}{8}$	2.72	1.58, 1.335, 1.10	1.338	18.08, -0.224, -17.788	0.995, 0.996, 0.996
$\frac{X_V}{7}$	2.73	1.59, 1.34, 1.10	1.343	18.39, -0.223, -18.093	0.995, 0.996, 0.996
$\frac{X_V}{6}$	2.74	1.60, 1.35, 1.105	1.3517	18.37, -0.126, -18.25	0.995, 0.996, 0.996
$\frac{X_V}{5}$	2.76	1.60, 1.35, 1.11	1.353	18.25, -0.221, -17.96	0.995, 0.996, 0.996
$\frac{X_V}{4}$	2.78	1.61, 1.36, 1.12	1.363	18.12, -0.22, -17.83	0.994, 0.995, 0.996
$\frac{X_V}{3}$	2.82	1.64, 1.38, 1.135	1.385	18.41, -0.36, -18.05	0.994, 0.995, 0.996
$\frac{X_V}{2}$	2.92	1.66, 1.42, 1.17	1.4167	17.17, 0.233, -17.41	0.994, 0.995, 0.996
X_V	Oscillatory	Oscillatory	—	—	Oscillatory

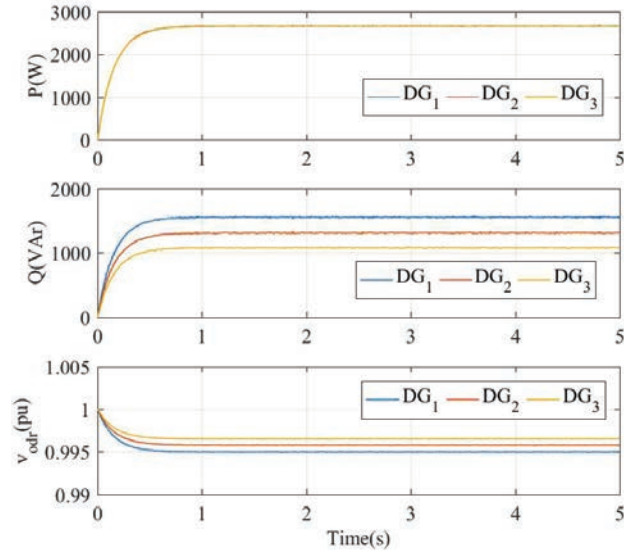


Figure 4 P/Q sharing and output voltages of DGs at $R_v = 0.0 \Omega$ and $X_v = 1.0 \Omega$ for common load case.

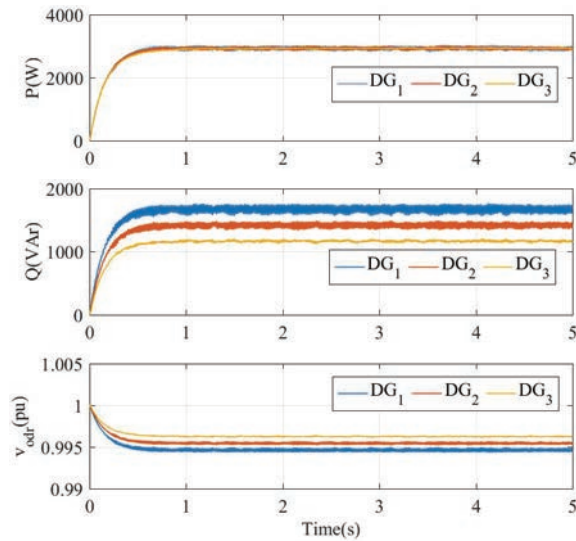


Figure 5 P/Q sharing and output voltages of DGs at $R_v = 0.0 \Omega$, $X_v = 1.0 \Omega$ and $X_{v_{add}} = \frac{X_v}{2} = 0.5 \Omega$ for common load case.

Table 4 Virtual impedance implementation for common plus local load case: $R_v = \text{constant}$, $X_v = \text{variable}$

Virtual impedance (Ω)	$P_{(1-3)}$ (kW)	$Q_{(1-3)}$ (kVAr)	Q_{exp} (kVAr)	$Q_{err(1-3)}$ (%)	$v_{odr(1-3)}$ (pu)
$R_v = 0, X_v = 0.1$	3.35	3.66, 1.17, 0.12	1.65	121.8, -29.1, -92.7	0.988, 0.996, 1.000
$R_v = 0, X_v = 0.2$	3.31	3.12, 1.31, 0.49	1.64	90.2, -20.1, -70.1	0.990, 0.996, 0.998
$R_v = 0, X_v = 0.3$	3.28	2.78, 1.37, 0.71	1.62	71.6, -15.4, -56.2	0.991, 0.995, 0.998
$R_v = 0, X_v = 0.4$	3.24	2.55, 1.40, 0.85	1.6	59.4, -12.5, -46.9	0.991, 0.996, 0.997
$R_v = 0, X_v = 0.5$	3.21	2.39, 1.42, 0.95	1.59	50.6, -10.5, -40.1	0.992, 0.996, 0.997
$R_v = 0, X_v = 0.6$	3.18	2.26, 1.43, 1.02	1.57	44.0, -8.9, -35.0	0.992, 0.995, 0.997
$R_v = 0, X_v = 0.7$	3.15	2.16, 1.43, 1.08	1.56	38.9, -8.0, -30.9	0.993, 0.995, 0.996
$R_v = 0, X_v = 0.8$	3.12	2.07, 1.43, 1.12	1.54	34.4, -7.1, -27.3	0.993, 0.995, 0.996
$R_v = 0, X_v = 0.9$	3.09	2.0, 1.43, 1.14	1.52	31.3, -6.1, -25.1	0.993, 0.995, 0.996
$R_v = 0, X_v = 1.0$	3.05	1.94, 1.42, 1.16	1.51	28.7, -5.7, -23.0	0.993, 0.995, 0.996
$R_v = 0, X_v = 1.1$	3.03	1.887, 1.422, 1.182	1.497	26.05, -5.01, -21.04	0.994, 0.995, 0.996
$R_v = 0, X_v = 1.2$	3.0	1.838, 1.413, 1.193	1.4813	24.08, -5.01, -21.04	0.994, 0.995, 0.996
$R_v = 0, X_v = 1.3$	2.97	1.793, 1.403, 1.202	1.466	22.30, -4.30, -18.0	0.994, 0.995, 0.996
$R_v = 0, X_v = 1.4$	2.935	1.751, 1.392, 1.207	1.45	20.76, -4.0, -16.76	0.994, 0.995, 0.996
$R_v = 0, X_v = 1.5$	2.905	1.714, 1.382, 1.210	1.4353	19.41, -3.71, -15.70	0.994, 0.995, 0.996

in reactive power sharing decreases and output voltage maintained at almost same value. The active power output decreases from $P = 3.35$ kW to $P = 2.905$ kW and reactive power output decreases from $Q_{exp} = 1.65$ kVAr to $Q_{exp} = 1.4353$ kVAr respectively (Table 4). Figure 6 also shows that active output power P and average reactive power Q_{exp} decreases when X_v is increased with virtual impedance technique which is downside of this technique. When modified virtual impedance technique is applied and the X_{vadd} increases, active and average reactive power starts improving and reaches at $P = 3.35$ kW and $Q = 1.64$ kVAr respectively at ($X_{vadd} = X_v/2$) while keeping reactive power sharing error and output voltage almost constant (refer Table 5, Figure 7).

So, it can be seen from comparative results of virtual impedance technique and modified virtual impedance technique that at higher value of X_v , Q_{err} is reduced but output power P and average reactive power (Q_{exp}) also reduces in case of virtual impedance technique compared to modified virtual impedance technique.

Table 5 Variation in $X_{V_{add}}$ keeping $R_V = 0.0$ and $X_V = 1.0$ for common plus local load case

$X_{V_{add}}$ (Ω)	$P_{(1-3)}$ (kW)	$Q_{(1-3)}$ (kVAr)	Q_{exp} (kVAr)	$Q_{err(1-3)}$ (%)	$v_{odr(1-3)}$ (pu)
$\frac{X_V}{10}$	3.10	1.97, 1.45, 1.185	1.535	28.34, -5.53, -22.80	0.993, 0.995, 0.996
$\frac{X_V}{9}$	3.11	1.975, 1.455, 1.185	1.5383	28.39, -5.41, -22.97	0.993, 0.995, 0.996
$\frac{X_V}{8}$	3.12	1.98, 1.455, 1.185	1.54	28.57, -5.52, -23.05	0.993, 0.995, 0.996
$\frac{X_V}{7}$	3.13	1.99, 1.46, 1.19	1.5467	28.66, -5.60, -23.06	0.993, 0.995, 0.996
$\frac{X_V}{6}$	3.15	1.99, 1.47, 1.195	1.5517	28.25, -5.27, -22.98	0.993, 0.995, 0.996
$\frac{X_V}{5}$	3.17	2.0, 1.475, 1.205	1.56	28.2, -5.45, -22.75	0.993, 0.995, 0.996
$\frac{X_V}{4}$	3.19	2.02, 1.49, 1.215	1.575	28.26, -5.40, -22.86	0.993, 0.995, 0.996
$\frac{X_V}{3}$	3.25	2.05, 1.51, 1.235	1.5983	28.26, -5.52, -22.73	0.993, 0.995, 0.996
$\frac{X_V}{2}$	3.35	2.10, 1.55, 1.27	1.64	28.05, -5.49, -22.563	0.993, 0.995, 0.996
X_V	Oscillatory	Oscillatory	—	—	Oscillatory

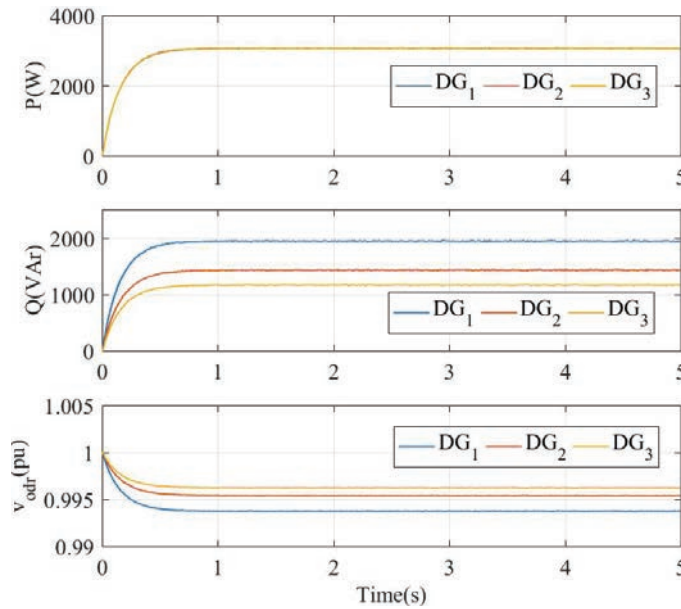


Figure 6 P/Q sharing and output voltages of DGs at $R_v = 0.0 \Omega$ and $X_v = 1.0 \Omega$ for common plus local load case.

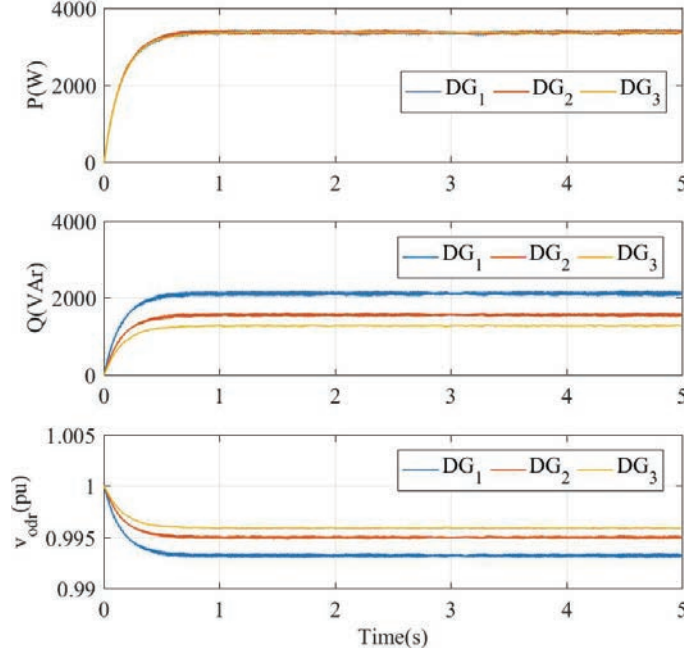


Figure 7 P/Q sharing and output voltages of DGs at $R_v = 0.0 \Omega$, $X_v = 1.0 \Omega$ and $X_{v_{add}} = \frac{X_v}{2} = 0.5 \Omega$ for common plus local load case.

4 Stability Analysis

To investigate the effect of modified virtual impedance control technique on the small signal stability margin of the system, the dynamic model of distributed generators operating in modified virtual impedance control scheme, lines and loads are firstly obtained separately and then are combined to obtain the complete dynamic model of microgrid which is expressed as:

$$\begin{bmatrix} \dot{\Delta X}_{INV} \\ \Delta I_{lineDQ} \\ \Delta I_{loadDQ} \end{bmatrix} = A_{mg} \begin{bmatrix} \Delta X_{INV} \\ \Delta I_{lineDQ} \\ \Delta I_{loadDQ} \end{bmatrix} \quad (3)$$

Where X_{INV} is states of all inverters. I_{lineDQ} and I_{loadDQ} are the states of all lines and loads respectively. There are thirteen states of the inverter: δ (angle between inverter reference frame and common reference frame), P (active power output), Q (reactive power output), ϕ_d (d-axis voltage flux), ϕ_q (q-axis voltage flux), γ_d (d-axis current flux), γ_q (q-axis current flux), i_{ld}

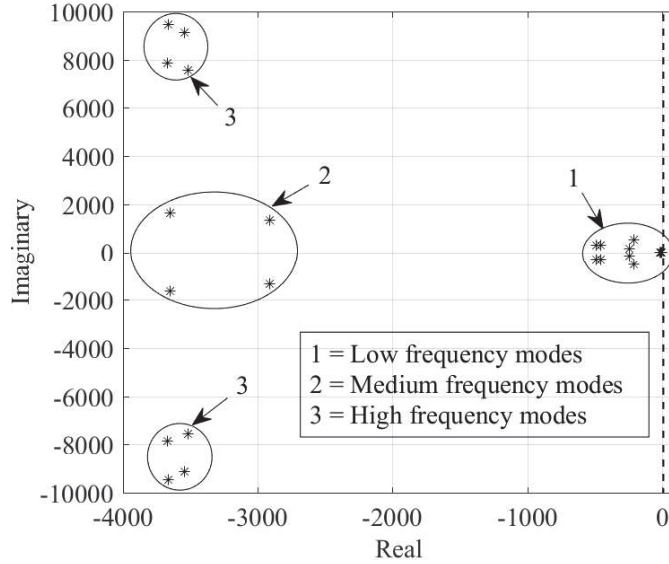


Figure 8 Eigenvalue plot with modified virtual impedance control.

(d-axis line current), i_{lq} (q-axis line current), v_{od} (d-axis output voltage), v_{oq} (q-axis output voltage), i_{od} (d-axis output current), i_{oq} (q-axis output current).

A_{mg} is state space matrix of complete system and its size is $(13s + 2n + 2p) \times (13s + 2n + 2p)$, where s number of sources, n is number of lines and p is number of loads connected to the system. In this manuscript the system under study has $s = 3$, $n = 3$, and $p = 1$ for common load case and $s = 3$, $n = 3$ and $p = 2$ for common plus local load case. Small signal stability analysis of the system (Figure 3) operating in modified virtual impedance technique is performed with the help of dynamic Equation (3). The steady state operating conditions of the system are obtained through MATLAB/Simulink. The complete eigenvalues of the system is shown in Figure 8. It is found that eigenvalues are mainly classified into three clusters including low frequency modes, medium frequency modes and high frequency modes Figure 8. The low frequency modes are mainly associated with the power controller state variables and the virtual impedances including R_v , X_v and $X_{v_{add}}$. The medium frequency modes are mainly associated with the state variables of voltage and current controllers and the high frequency modes are mainly associated with the LC filter with coupling inductor.

Eigenvalue trace by varying the value of m_p (0.00005:0.00005:0.003) for $R_v = 0.0 \Omega$, $X_v = 1.0 \Omega$, $X_{v_{add}} = 0.1 \Omega$ and $n_q = 1.0 \times 10^{-4} \text{ V/(VAR)}$ is

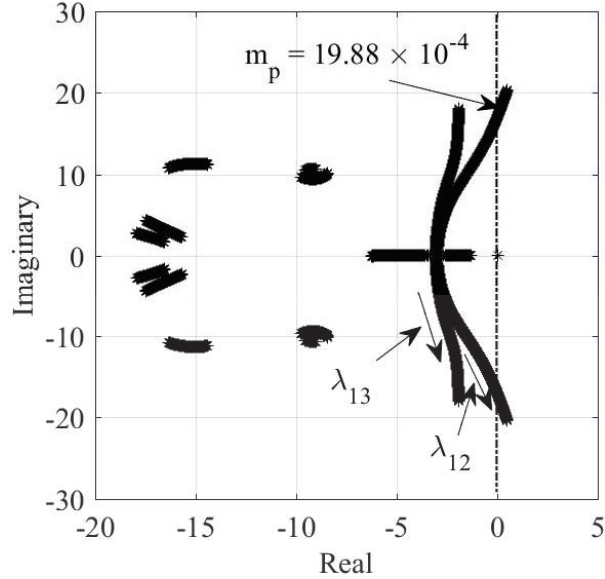


Figure 9 Eigenvalue trace for low frequency modes with modified virtual impedance control: $0.00005 \leq m_p \leq 0.003$.

obtained and shown in Figure 9. It is found that λ_{12} and λ_{13} are most sensitive eigenvalues subjected to system stability and are related to the low frequency modes of inverter 1–2 and inverter 1–3 respectively. It is also found that λ_{12} reaches the imaginary axis before λ_{13} at the of $m_p = 19.88 \times 10^{-4}$.

Eigenvalue trace by varying the value of n_q (0.0001:0.0001:0.007) for $R_v = 0.0 \Omega$, $X_v = 1.0 \Omega$, $X_{v_{add}} = 0.1 \Omega$ and $m_p = 5.0 \times 10^{-5} \text{ rad}/(\text{W.s})$ is obtained and shown in Figure 10. It is found that λ_{12} and λ_{13} are most sensitive eigenvalues subjected to system stability and are related to the low frequency modes of inverter 1-2 and inverter 1-3 respectively. It is also found that λ_{12} reaches the imaginary axis before λ_{13} at the of $n_q = 56.68 \times 10^{-4}$.

Effect on the stability margin of the system for modified virtual impedance control (Equation 2) is studied and compared with the stability margin obtained with conventional virtual impedance control. The study is performed in the following manner:

- Effect of variation in X_v (0.1:0.1:1.0 Ω) for the values of $R_v = 0.0$ and 0.1Ω respectively is studied for conventional virtual impedance control and value of $m_{p,max}$ is obtained at $n_q = 1.0 \times 10^{-4} \text{ V}/(\text{VAr})$ which is depicted in Table 6.

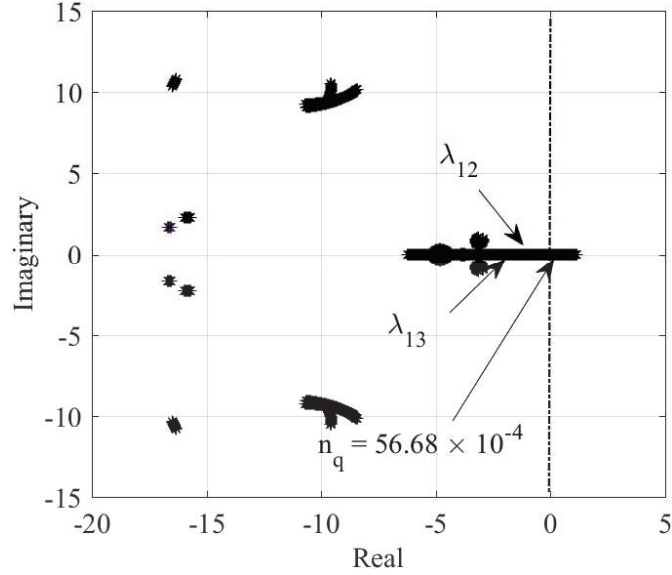


Figure 10 Eigenvalue trace for low frequency modes with modified virtual impedance control: $0.0001 \leq n_q \leq 0.007$.

Table 6 Effect of variation in R_v and X_v on $m_{p,max}$ for conventional virtual impedance technique at $n_q = 1.0 \times 10^{-4}$ V/(VAr)

Virtual impedance (Ω)	$m_{p,max}$ rad/(W.s)	Virtual impedance (Ω)	$m_{p,max}$ rad/(W.s)
$R_v = 0, X_v = 0.1$	1.96×10^{-4}	$R_v = 0.1, X_v = 0.1$	3.76×10^{-4}
$R_v = 0, X_v = 0.2$	1.79×10^{-4}	$R_v = 0.1, X_v = 0.2$	3.08×10^{-4}
$R_v = 0, X_v = 0.3$	2.02×10^{-4}	$R_v = 0.1, X_v = 0.3$	3.13×10^{-4}
$R_v = 0, X_v = 0.4$	2.52×10^{-4}	$R_v = 0.1, X_v = 0.4$	3.58×10^{-4}
$R_v = 0, X_v = 0.5$	3.29×10^{-4}	$R_v = 0.1, X_v = 0.5$	4.37×10^{-4}
$R_v = 0, X_v = 0.6$	4.44×10^{-4}	$R_v = 0.1, X_v = 0.6$	5.57×10^{-4}
$R_v = 0, X_v = 0.7$	6.15×10^{-4}	$R_v = 0.1, X_v = 0.7$	7.48×10^{-4}
$R_v = 0, X_v = 0.8$	8.81×10^{-4}	$R_v = 0.1, X_v = 0.8$	10.52×10^{-4}
$R_v = 0, X_v = 0.9$	13.38×10^{-4}	$R_v = 0.1, X_v = 0.9$	16.06×10^{-4}
$R_v = 0, X_v = 1.0$	21.72×10^{-4}	$R_v = 0.1, X_v = 1.0$	27.36×10^{-4}

Table 7 Effect of variation in R_v and X_v on $n_{q,max}$ for conventional virtual impedance technique at $m_p = 5.0 \times 10^{-5}$ rad/(W.s)

Virtual impedance (Ω)	$n_{q,max}$ V/(VAr)	Virtual impedance (Ω)	$n_{q,max}$ V/(VAr)
$R_v = 0, X_v = 0.1$	8.85×10^{-4}	$R_v = 0.1, X_v = 0.1$	9.88×10^{-4}
$R_v = 0, X_v = 0.2$	14.13×10^{-4}	$R_v = 0.1, X_v = 0.2$	14.84×10^{-4}
$R_v = 0, X_v = 0.3$	19.57×10^{-4}	$R_v = 0.1, X_v = 0.3$	20.02×10^{-4}
$R_v = 0, X_v = 0.4$	24.85×10^{-4}	$R_v = 0.1, X_v = 0.4$	25.13×10^{-4}
$R_v = 0, X_v = 0.5$	30.18×10^{-4}	$R_v = 0.1, X_v = 0.5$	30.88×10^{-4}
$R_v = 0, X_v = 0.6$	35.47×10^{-4}	$R_v = 0.1, X_v = 0.6$	36.02×10^{-4}
$R_v = 0, X_v = 0.7$	40.73×10^{-4}	$R_v = 0.1, X_v = 0.7$	41.17×10^{-4}
$R_v = 0, X_v = 0.8$	46.06×10^{-4}	$R_v = 0.1, X_v = 0.8$	46.91×10^{-4}
$R_v = 0, X_v = 0.9$	51.36×10^{-4}	$R_v = 0.1, X_v = 0.9$	51.56×10^{-4}
$R_v = 0, X_v = 1.0$	56.57×10^{-4}	$R_v = 0.1, X_v = 1.0$	56.84×10^{-4}

- Effect of variation in X_v (0.1:0.1:1.0 Ω) for the values of $R_v = 0.0$ and 0.1Ω respectively is studied for conventional virtual impedance control and value of $n_{q,max}$ is obtained at $m_p = 5.0 \times 10^{-5}$ rad/(W.s) which is depicted in Table 7.
- Effect of variation in $X_{v_{add}}$ (0.1:0.1:1.0 Ω) on $m_{p,max}$ is studied for modified virtual impedance technique at $R_v = 0.0 \Omega$, $X_v = 1.0 \Omega$, $n_q = 1.0 \times 10^{-4}$ V/(VAr) which is depicted in Table 8.
- Effect of variation in $X_{v_{add}}$ (0.1:0.1:1.0 Ω) on $n_{q,max}$ is studied for modified virtual impedance technique at $R_v = 0.0 \Omega$, $X_v = 1.0 \Omega$, $m_p = 5.0 \times 10^{-5}$ rad/(W.s) which is depicted in Table 9.

The findings of the results are as follows:

- For the conventional virtual impedance control, the value of $m_{p,max}$ increases with the increasing value of X_v except for the value of $X_v = 0.2 \Omega$ when n_q are kept constant (refer to Table 6).
- For the conventional virtual impedance control, the value of $n_{q,max}$ increases with the increasing value of X_v when m_p are kept constant (refer to Table 7).
- For the modified virtual impedance control, the value of $m_{p,max}$ decreases with the increasing value of $X_{v_{add}}$ when R_v , X_v and n_q are kept constant (refer to Table 8).

Table 8 Effect of variation in $X_{v_{add}}$ on $m_{p,max}$ for modified virtual impedance technique at $R_v = 0.0 \Omega$, $X_v = 1.0 \Omega$, $n_q = 1.0 \times 10^{-4}$ V/(VAr)

$X_{v_{add}}$ (Ω)	$m_{p,max}$ rad/(W.s)	$X_{v_{add}}$ (Ω)	$m_{p,max}$ rad/(W.s)
0.1	19.88×10^{-4}	0.6	12.04×10^{-4}
0.2	18.17×10^{-4}	0.7	10.76×10^{-4}
0.3	16.37×10^{-4}	0.8	9.46×10^{-4}
0.4	14.88×10^{-4}	0.9	8.22×10^{-4}
0.5	13.33×10^{-4}	1.0	Oscillatory

Table 9 Effect of variation in $X_{v_{add}}$ on $n_{q,max}$ for modified virtual impedance technique at $R_v = 0.0 \Omega$, $X_v = 1.0 \Omega$, $m_p = 5.0 \times 10^{-5}$ rad/(W.s)

$X_{v_{add}}$ (Ω)	$n_{q,max}$ V/(VAr)	$X_{v_{add}}$ (Ω)	$n_{q,max}$ V/(VAr)
0.1	56.68×10^{-4}	0.6	57.38×10^{-4}
0.2	56.82×10^{-4}	0.7	57.47×10^{-4}
0.3	56.98×10^{-4}	0.8	57.53×10^{-4}
0.4	57.13×10^{-4}	0.9	57.67×10^{-4}
0.5	57.27×10^{-4}	1.0	Oscillatory

- For the modified virtual impedance control, the value of $n_{q,max}$ remains almost constant with the increasing value of $X_{v_{add}}$ when R_v , X_v and m_p are kept constant (refer to Table 9).

5 Conclusion

The proposed modified virtual impedance control bring back the sum of real and reactive power output of all the distributed generators to the nominal value. The proposed technique is based on insertion of an additional term ($-X_{v_{add}}I_{od}$) in d-axis component of virtual impedance voltage keeping q-axis component unchanged so as to keep the reactive power sharing error almost constant for different values of $X_{v_{add}}$. The proposed method is simulated in MATLAB/Simulink environment and found suitable for different network configurations. Small signal stability analysis is performed and it is found that the proposed control scheme reduces the system stability. Improvement in the stability margin of the system with the modified virtual impedance technique is the scope of future work.

References

- [1] D. K. Dheer, Y. Gupta, and S. Doolla, "Decentralized inverter control for improved reactive power sharing and voltage profile in a microgrid," *IET Gen., Trans. and Dist.*, vol. 15, no. 7, pp. 1227–1241, 2021.
- [2] N. Pogaku, M. Prodanovic, and T. C. Green, "Modeling, analysis and testing of autonomous operation of an inverter-based microgrid," *IEEE Trans. Power Electron.*, vol. 22, no. 2, pp. 613–625, March 2007.
- [3] D. E. Olivares, A. Mehrizi-Sani, A. H. Etemadi, C. A. Cañizares, R. Iravani, M. Kazerani, A. H. Hajimiragha, O. Gomis-Bellmunt, M. Saeedifard, R. Palma-Behnke, G. A. Jiménez-Estévez and N. D. Hatziargyriou, "Trends in Microgrid Control," *IEEE Trans. Smart Grid.*, vol. 5, no. 4, pp. 1905–1919, July 2014.
- [4] Qing-Chang Zhong, "Robust Droop Controller for Accurate Proportional Load Sharing Among Inverters Operated in Parallel," *IEEE Trans. Ind. Electron.*, vol. 60, no. 4, pp. 1281–1290, Apr. 2013.
- [5] M. V. Kazemi, S. J. Sadati, and S. A. Gholamian, "Adaptive Frequency Control of Microgrid Based on Fractional Order Control and a Data-Driven Control With Stability Analysis," *IEEE Trans. Smart Grid.*, vol. 13, no. 1, pp. 381–392, Jan. 2022.
- [6] D. K. Dheer, Y. Gupta, and S. Doolla, "A Self-Adjusting Droop Control Strategy to Improve Reactive Power Sharing in Islanded Microgrid," *IEEE Trans. Sust. Energy.*, vol. 11, no. 3, pp. 1624–1635, Jan. 2020.
- [7] Y. Gupta, K. Chatterjee, and S. Doolla, "A Simple Control Scheme for Improving Reactive Power Sharing in Islanded Microgrid," *IEEE Trans. Power System.*, vol. 35, no. 4, pp. 3158–3169, Jul. 2020.
- [8] Y. Qi, J. Fang, and Y. Tang, "Utilizing the Dead-Time Effect to Achieve Decentralized Reactive Power Sharing in Islanded AC Microgrids," *IEEE Trans. Emer. and Select. topic in Power Electron.*, vol. 8, no. 3, pp. 2350–2361, Sep. 2020.
- [9] J. Lu, X. Zhang, B. Zhang, Xi. Hou, and P. Wang, "Distributed Dynamic Event-Triggered Control for Voltage Restoration and Current Sharing in DC Microgrids," *IEEE Trans. Sust. Energy*, vol. 13, no. 1, pp. 619–628, Jan. 2022.
- [10] J. He, Y. W. Li, "Analysis and Design of Interfacing Inverter Output Virtual Impedance in A Low Voltage Microgrid," in *Proc. IEEE Energy Conversion Congress and Exposition.*, pp. 2857–2864, 2010

- [11] J. He, and Y. W. Li, "Analysis, Design, and Implementation of Virtual Impedance for Power Electronics Interfaced Distributed Generation," *IEEE Trans. Indus. App.*, vol. 47, no. 6, pp. 2525–2238, Dec. 2011.
- [12] R. J. Wai, Q. Q. Zhang, and Y. Wang, "A Novel Voltage Stabilization and Power Sharing Control Method Based on Virtual Complex Impedance for an Off-Grid Microgrid," *IEEE Trans. Power Electron.*, vol. 34, no. 2, pp. 1863–1880, Feb. 2019.
- [13] W. Deng, N. Dai, K. W. Lao, and J. M. Guerrero, "A Virtual-Impedance Droop Control for Accurate Active Power Control and Reactive Power Sharing Using Capacitive-Coupling Inverters," *IEEE Trans. Indus. App.*, vol. 56, no. 6, pp. 6722–6733, Nov. 2020.
- [14] Y. Zhu, F. Zhuo, F. Wang, B. Liu, R. Gou, and Yangjie Zhao, "A Virtual Impedance Optimization Method for Reactive Power Sharing in Networked Microgrid," *IEEE Trans. Power Electron.*, vol. 31, no. 4, pp. 2890–2904, Apr. 2016.
- [15] B. Pournazarian, S. S. Seyedalipour, M. Lehtonen, S. Taheri, and E. Pouresmaeil, "Virtual Impedances Optimization to Enhance Microgrid Small-Signal Stability and Reactive Power Sharing," *IEEE Access.*, vol. 8, pp. 139691–139705, July. 2020.
- [16] M. D. Pham and H. H. Lee, "Effective Coordinated Virtual Impedance Control for Accurate Power Sharing in Islanded Microgrid," *IEEE Trans. Indus. Electron.*, vol. 68, no. 3, pp. 2279–2288, Mar. 2021.
- [17] Tuan V. Hoang and Hong-Hee Lee, "An Adaptive Virtual Impedance Control Scheme to Eliminate the Reactive-Power-Sharing Errors in an Islanding Meshed Microgrid," *IEEE Trans. Emer. and Select. topic in Power Electron.*, vol. 6, no. 2, pp. 966–976, June. 2018.
- [18] Z. Li, K. W. Chan, J. Hu, and Josep M. Guerrero, "Adaptive Droop Control Using Adaptive Virtual Impedance for Microgrids With Variable PV Outputs and Load Demands," *IEEE Trans. Indus. Electron.*, vol. 68, no. 10, pp. 9630–9640, Oct. 2021.
- [19] S. Khanabdal, M. Banejad, F. Blaabjerg and N. Hosseinzadeh, "Adaptive Virtual Flux Droop Control based on Virtual Impedance in Islanded AC Microgrids," *IEEE Journal of Emerging and Selected Topics in Power Electron.*, Early access article.
- [20] M. Ahmed, L. Meegahapola, A. Vahidnia and M. Datta, "Adaptive Virtual Impedance Controller for Parallel and Radial Microgrids with Varying X/R Ratios," *IEEE Transactions on Sustainable Energy*, Early access article.

Biographies



Pradeep Kumar Singh. He is born in Kushinagar, UP, India. He received the B.Tech. degree in electrical engineering from UPTU Lucknow, India, in 2007, the M.Tech. degree in control and instrumentation with specialization voltage regulation from National Institute of Technology Jalandhar, India, in 2009. Currently he is Ph.D scholar at the department of electrical engineering, National Institute of Technology Patna, Bihar. He has 10 years of experience in the field of teaching, research. His current research interest includes microgrid operations and control.



Dharmendra Kumar Dheer. He is born in Bhagalpur, Bihar, India. He received the B.Sc. engineering degree in electrical engineering from Muzaffarpur Institute of Technology Muzaffarpur, India, in 2007, the M.Tech. degree in electrical engineering with specialization in power system engineering from Indian Institute of Technology Kharagpur, India, in 2010, and the Ph.D. degree in power and energy systems engineering from the department of Energy Science and Engineering, Indian Institute of Technology Bombay, Mumbai, India, in 2017. Currently he is serving as an assistant professor at the department of electrical engineering, National Institute of Technology Patna,

Bihar. He has one and half year of teaching experience after M.Tech. degree, six month of research experience as a research associate at IIT Bombay and five and half months of research experience as a postdoctoral researcher at Arizona State University (ASU), USA. His current research interest includes stability and control of microgrids, stability aspects of conventional power systems, active distribution network and solar photovoltaic.